

# The boundary force exerted on spatial solitons in cylindrical strongly nonlocal media

Qian Shou, Yanbin Liang, Qun Jiang, Yajian Zheng, Sheng Lan, Wei Hu\* and Qi Guo\*

Laboratory of Photonic Information Technology, South China Normal University, Guangzhou, 510631, China

\*Corresponding author: huwei@scnu.edu.cn, guoq@scnu.edu.cn

Compiled November 5, 2018

We investigate the propagation of the spatial soliton in cylindrical strongly nonlocal media by a novel method of image beam of light. The effect of the boundary on the soliton acting as the dynamic force for the soliton steering is equivalent to the force between the soliton beam and the image beam. The trajectory of the soliton is analytically studied which is in good agreement with the experimental results. © 2018 Optical Society of America

OCIS codes: 190.0190

Nonlocal spatial solitons are extensively investigated[1-16] since the pioneering work of Snyder and Mithcell[1]. A topic that has captured a rising interest is the interaction between solitons and the boundaries[4-8], especially in lead glass. The group of Morderchai Segev found the boundary caused elliptic solitons and vortex solitons in lead glass and discussed the influence of the boundary force on the soliton trajectory[5,6]. In liquid crystal A. Alberucci et al demonstrated the power-depended soliton repulsion at the boundary[7,8]. The nonlocal nature of lead glass lies in the thermal optical nonlinearity (Poisson type) which is intrinsically infinite without boundaries[5]. Therefore the behavior of the nonlocal solitons in lead glass can be greatly influenced by the remote boundary and one can easily obtain solitons output controlled by asymmetric boundary forces[6]. In addition, the problem of light trajectory is generally settled by the method of equivalent particle theory and light ray equation[6,17] since the beam width is quite less than the media size. The particle behavior of light suggests that the soliton can be taken as a point light on the cross section of the propagation media.

In this paper by analogy with the method of images in electrostatics, we introduce a method of image beam of light to deal with the problem of the boundary effect on the soliton trajectory in cylindrical lead glass. The boundary force exerted on the soliton can be equivalent to the force of a remote image point light to the soliton. The experimental data of soliton steering can be fitted by analytical solution in good agreement.

The system we concern is the light-induced thermal self-focusing nonlinearity in lead glass. The heat energy of the light is slightly absorbed with an absorption coefficient  $\alpha$  and diffused with a thermal conductivity  $\kappa$ . The cylindrical boundary of the lead glass is thermally contacted by a heat sink at a fixed temperature  $T_0$  described by Fig. 1(a). A temperature gradient is yielded

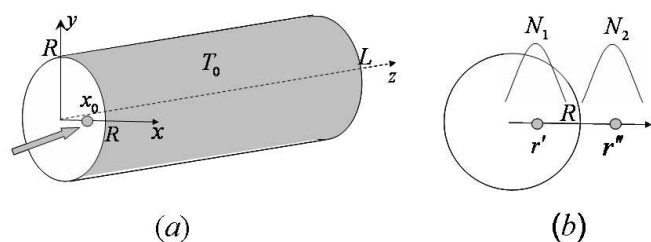


Fig. 1. (a) Diagrammatic layout of a soliton launched at an offset of  $x_0$  in a circular cross section of the sample with radius  $R$ . (b) Sketch map of the normalized refractive indexes respectively induced by the source beam and the image beam.

whose distribution is governed by Poisson equation[5]:

$$\begin{aligned} \nabla^2 T(X, Y) &= -\frac{\alpha}{\kappa} I(X, Y) \\ T(X, Y)|_{X^2+Y^2=R^2} &= T_0, \end{aligned} \quad (1)$$

where  $T(X, Y)$  is the temperature distribution,  $I(X, Y) = |A(X, Y)|^2$  is the light intensity with  $A(X, Y)$  being the paraxial beam and  $R$  is the radius of the cylinder cross section. The heat transfer equation is inherently two-dimensional with circular boundary as the soliton is invariant in the direction of propagation. The laser-induced temperature change  $\Delta T = T - T_0$  gives rise to a proportional increase in refractive index[5]  $\Delta n = \beta \Delta T$  with the thermo-optical coefficient  $\beta$ , and in reverse the refractive index change has a strong impact on the propagation characteristics of the light beam, including the focusing and the steering. The propagation of an optical beam in lead glass is moded by Equation (1) coupled with the equation for the paraxial beam  $A(X, Y)$ :

$$\nabla^2 A + 2ik \frac{\partial A}{\partial z} + 2k^2 \frac{\Delta n}{n_0} A = 0, \quad (2)$$

where  $k$  is the wave vector. We rewrite Eq. (1) and (2)

in a dimensionless form:

$$\begin{aligned} i\partial_z\varphi + \frac{1}{2}\nabla_{\perp}^2\varphi + N\varphi &= 0 \\ \nabla_{\perp}^2 N &= -|\varphi|^2 \\ N(x, y)|_{x^2+y^2=1} &= 0, \end{aligned} \quad (3)$$

where the normalized coordinates and functions are setting as:  $x = X/R, y = Y/R, z = Z/(kR^2), \varphi = A/A_0$  with  $A_0^2 = n_0\kappa/(\alpha\beta k^2 R^2)$  and  $N = k^2 R^2 \Delta n/n_0$ . It is noticeable that  $N$  and  $|\varphi|^2$  in Eq. 3(b) have their counterparts in electrostatics, potential and charges respectively.

We solve the light-induced refractive index distribution in the view of Green function method. In circular domain, the Green function of Poisson equation can be deduced by the method of images[18] which is the sum potential of the source charge and the image charge:

$$G = \frac{1}{2\pi} \left( \ln \frac{1}{|\mathbf{r} - \mathbf{r}'|} - \ln \frac{r''}{|\mathbf{r} - \mathbf{r}''|} \right) = G_1 + G_2, \quad (4)$$

where  $\mathbf{r}(x, y), \mathbf{r}'(x', y')$  and  $\mathbf{r}''(x'', y'')$  are respectively the normalized radius vectors of the field point, the source point and the image point and  $r'' = 1/r'$  described in Fig. 1(b). The image charge simulates the influence of all the inductive charges on the boundary, so the force applied to the source charge by the boundary is equivalent to the force between the image charge and the source charge. In our present case, when the source light has a beam width small enough compared with the boundary size, it can be taken as a point light beam. Borrowing ideas from the method of images in the electrostatics we introduce the method of image beam of light. By analogy with the the expression of the charge interaction, we directly write the “force” between the source and image beams which provides the dynamic force for the steering of the source beam:

$$f = \frac{d^2 x_c}{dz^2} \propto \frac{p}{1/x_c - x_c}, \quad (5)$$

where  $(x_c, 0)$  is the source beam center,  $(1/x_c, 0)$  is the image beam center and  $y$  has been set zero since the problem is  $y$ -symmetric.  $p = \int |\varphi(x' - x_c, y')|^2 dx' dy'$  is the normalized light power which is equivalent to the charge density in electrostatics. The  $1/r$  law of interaction is ever predicted by C. Rostschild et al[3].

The interaction of the two beams is mediated by the light-induced index which is the solution of Eq. 3(c). When we make further quantitative analysis, the solution is given by:

$$\begin{aligned} N &= \frac{1}{2\pi} \int (G_1 + G_2) |\varphi(x' - x_c, y')|^2 dx' dy' \\ &= N_1 + N_2. \end{aligned} \quad (6)$$

The integration has been expressed in two terms of  $N_1$  and  $N_2$ .  $N_1$  is symmetric about the beam center  $(x_c, 0)$  since  $G_1$  is shift invariant and the beam has a symmetric

profile(in the general case). It represents the source beam induced refractive index in the free space who inversely serves as the focusing lens for the source beam to form solitons. We can obtain the critical power of the soliton  $P_c = 4\pi n_0 \kappa / (\alpha \beta k^2 w_0^2)$  with  $w_0$  being the beam width by expanding  $N_1$  to the second order[19]. The effect of  $N_2$  on the source beam is equivalent to the effect of the refractive index induced by the image beam located at the image point  $(1/x_c, 0)$  indicated in Fig. 1(b).

In the case of  $w_0 \ll R$ ,  $G_2$  is almost unchanged in the profile of the light beam,  $N_2$  reads

$$\begin{aligned} N_2 &= -\frac{1}{2\pi} \int \ln \frac{r''}{|r - r''|} |\varphi(x' - x_c, y')|^2 dx' dy' \\ &= -\frac{p}{2\pi} \ln \frac{1/x_c}{\sqrt{(x - 1/x_c)^2 + y^2}}. \end{aligned} \quad (7)$$

The steering trajectory of a light ray is governed by the Eikonal equation[9,17]:

$$\frac{d^2 x_c}{dz^2} = \frac{dN_2}{dx} \Big|_{x=x_c, y=0} = -\frac{p}{2\pi} \frac{1}{1/x_c - x_c}. \quad (8)$$

Just as our qualitative anticipation in Eq. (5), the acceleration of the source beam center has a form analogous to that of the inter-force between the source and the image charges. We expand the right hand side of Eq. (8) with respect to  $x_c$  about  $x_c = 0$  under the condition of  $x_c \ll 1$ :

$$\frac{d^2 x_c}{dz^2} = -\frac{p}{2\pi} (x_c + x_c^3 + x_c^5). \quad (9)$$

We only provide the solution under the first-order approximation since the solutions under the third and fifth-order approximations containing Jacobi cn functions are too long to be showed:

$$x_c^{(z)} = x_{c0} \cos\left(\sqrt{\frac{p}{\pi}} z\right), \quad (10)$$

where  $x_{c0}$  is the normalized input offset. The normalized output coordinate  $x_c^{(l)}$ , where  $l$  is the normalized length of the lead glass, is proportional to  $x_{c0}$  when the input light power maintains constant.

Fig. 2(a) pictures the theoretical period of the beam steering versus the input offset. The period decreases when the input offset approaches the boundary. This is understandable since strong boundary effect accelerates the oscillation of the beam. Nevertheless the oscillation period is too long compared to our glass length even in the strong acceleration case. Fig. 2(b) is the beam oscillation at the input offset of  $0.8R$ .

Our experimental setup is similar to that for the work of B. Alfassi et al[6]. The sample is a cylindrical heavily lead-doped glass sample with the radius  $R = 1.5$  mm and length  $L = 5$  cm (Fig. 1(a)). The absorption coefficient  $\alpha = 0.07$  cm<sup>-1</sup>, the thermo-optical coefficient  $\beta = 14 \times 10^{-6}$  K<sup>-1</sup>, the refractive index  $n_0 = 1.9$  and the thermal conductivity  $\kappa = 0.7$  W/(mK). The 50  $\mu$ m FWHM light input is produced by a double frequency

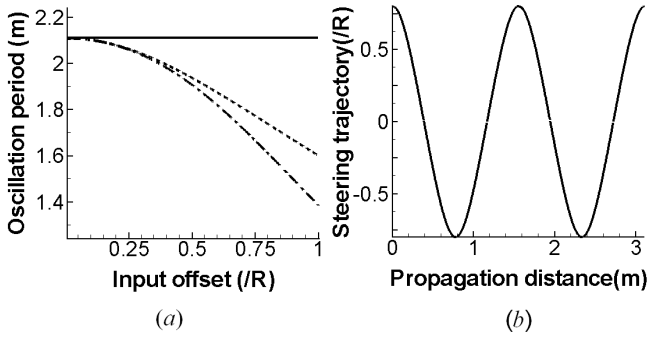


Fig. 2. (a) The theoretical oscillation period versus the input offset. Solid line: first order approximation. Solid line: first order approximation; dashed line: third order approximation; dashdotted line: fifth order approximation. (b) The theoretical period of the beam steering versus the input offset under the fifth approximation.

YAG laser(Verdi 5) with the wavelength 532 nm. The soliton critical power is measured to be 500  $mW$  which is in good agreement with the analytical value[19] under the experimental parameters. The data of the steering experiment are obtained under the higher light power of 700  $mW$ . Fig. 4 gives the comparisons between the experimental data and the theoretical fitting curves. The first approximation solution is a straight line, it can be fitted to the experimental data only when the input offset is small enough. The higher order approximation gives the better agreement with the experimental result. It is noticeable that the propagation distance in Fig. 2(b) is far longer than the actual sample size. Yet we can not obtain large steering via lengthening the glass or obtain the output at the desired period, because the absorption will result in the changing of the beam width even the collapse of the soliton.

In conclusion, the soliton propagation in cylindrical lead glass is studied. A novel method of image beam of light is produced by analogy with the method of images in electrostatics. The boundary effect on the soliton is treated as the inter-force between the soliton beam and the image beam located at the image point. The analytical solution of the soliton trajectory is in good agreement with the experimental results. The method of image beam of light is useful in the treatment of the boundary problems, including the influence of the boundary force on the soliton trajectory and even the interaction between solitons via the boundary effect.

This research was supported by the National Natural Science Foundation of China (Grant Nos. 10804033 and 10674050) and Program for Innovative Research Team of the Higher Education in Guangdong (Grant No. 06CXTD005).

## References

1. A. W. Snyder and D. J. Mitchell, *Science* **276**, 1538 (1997).

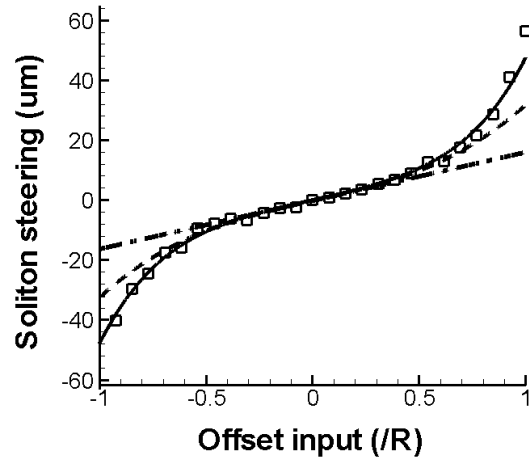


Fig. 3. A net steering relative to the input offset versus the input offset. Squares: the experimental result; dash-dotted line: the first approximation solution  $x_{c0} - x_c^{(1)}$ ; dashed line: the third approximation solution  $x_{c0} - x_c^{(3)}$ ; solid line: the fifth approximation solution  $x_{c0} - x_c^{(5)}$ .

2. C. Rotschild, M. Segev, Z. Y. Xu, Y. V. Kartashov and L. Torner, *Opt. Lett.* **31**, 3312-3314 (2006).
3. C. Rotschild, B. Alfassi, O. Cohen and M. Segev, *Nature Physics* **2**, 769 (2006).
4. B. Alfassi, C. Rotschild, O. Manela, M. Segev and D. N. Christodoulides, *Phys. Rev. Lett.* **98**, 213901 (2008).
5. C. Rotschild, O. Cohen, O. Manela and M. Segev, *Phys. Rev. Lett.* **95**, 213904-4 (2005).
6. B. Alfassi, C. Rotschild, O. Manela and M. Segev, *Opt. Lett.* **32**, 154-156 (2007).
7. A. Alberucci, M. Peccianti and Gaetano Assanto, *Opt. Lett.* **32**, 2795 (2002).
8. A. Alberucci and G. Assanto, *J. Opt. Soc. Am. B* **24**, 2314 (2007).
9. M. Peccianti, A. De Rossi, G. Assanto, A. De Luca, C. Umerton and I. C. Khoo, *Appl. Phys. Lett.* **77**, 7 (2000).
10. Marco Peccianti, Katarzyna A. Brzdakiewicz, and G. Assanto, *Opt. Lett.* **27**, 1460 (2002).
11. Claudio Conti, Marco Peccianti, and Gaetano Assanto, *Phys. Rev. Lett.* **91**, 073901 (2003).
12. Marco Peccianti, Claudio Conti, Gaetano Assanto et al., *Nature*, **432**, 733 (2004).
13. Q. Guo, B. Luo, F. H. Yi, S. Chi and Y. Q. Xie, *Phys. Rev. E* **69**, 016602 (2004).
14. W. Hu, T. Zhang, Q. Guo, L. Xuan and S. Lan, *Appl. Phys. Lett.* **89**, 071111 (2006).
15. Z. P. Dai, Y. Q. Wang and Q. Guo, *Phys. Rev. A* **77**, 063834 (2008).
16. D. M. Deng and Q. Guo, *Opt. Lett.* **32**, 3206 (2007).
17. A. B. Aceves, J. V. Moloney and A. C. Newell, *Phys. Rev. A*, **39**, 1809 (1988).
18. John Dabvid Jackson, *Classical electrodynamics*,
19. Y. B. Liang, Y. J. Zheng, P. B. Yang, L. G. Cao, D. Q. Lu, W. Hu and Q. Guo, *Acta Phys. Sin.(in Chinese)* **57**, 5690(2008).